Kinetics analysis of copper complex photoredox catalyst: roles of oxygen, thickness, and optimal concentration for radical/cationic hybrid photopolymerization

Jui-Teng Lin[1,*], Jacques Lalevee[2] and Da-Chun Cheng[3,*]

. [1] New Vision Inc., 10F, No. 55, Sect.3, Xinbei Blvd, Xinzhuang, New Taipei City, Taiwan; jtlin55@gmail.com 5

. [2] Université de Haute-Alsace, CNRS, IS2M UMR 7361, F-68100 Mulhouse, France; jacques.lalevee@uha.fr 6

. [3] Department of of Biomedical Imaging and Radiological Science, China Medical University, 404, Taiwan, 7 ROC; dccheng@mail.cmu.edu.tw

* Correspondences: jtlin55@gmail.com; dccheng@mail.cmu.edu.tw

. **Abstract**

. This article presents, for the first time, the kinetics and the general conversion features of a 3-initiator system (A/B/N), based on proposed mechanism of Mokbel et al, for both free radical polymerization (FRP) of acrylates and the free radical promoted cationic polymerization (CP) of epoxides using copper complex as the initiator. Higher FRP and CP conversion can be achieved by co-initiators concentration [B] and [N], via the dual function of (i) regeneration [A], and (ii) generation of extra radicals S' and S. The FRP and CP conversion is proportional to, respectively, the nonlinear and linear power of bI[A][B], where b and I are the absorption coefficient and the light intensity, respectively. System in air has lower conversion than in laminate due to the oxygen inhibition effects. For thick samples (with thickness z), there is an optimal concentration [A*] which is inverse proportional (bzI), in contrast with very thin sample, in which the conversion is an increasing function of [A] and [B]. The unique feature of dark polymerization in CP conversion enables the polymerization to continue in living mode, in contrasts with that of the radical-mediated pathway in most conventional FRP. The measured results of Mokbel et al are well analyzed and matching the predicted features of our modeling.

. **Keywords:** polymerization kinetics; photoinitiator; free radical, cationic polymerization, copper complex, photoredox catalyst.

1. Introduction

Light sources from UV (365 nm) to near-infrared (980 nm) have been used for photopolymerization reactions in many industrial and medical applications such as dental curing, microlithography, stereolithography, microelectronics, holography [1,2]. Variety of photoresponsive materials such as conjugated polymers have been reported for additive manufacturing (AM) and recently for 3D and 4D bioprinting [3-7]. Both spatial and temporal controlled 3D processes were reported using single and multiple wavelength lights [6-11]. The reported conversion enhancing methods include the use of novel materials as enhancers or co initiators in both single and multiple components [9-10]. Two stage polymerization under two wavelengths to eliminate the oxygen inhibition effects was also reported experimentally [11]. Sequential network formation has also been

achieved with many different types of polymerization methods, such as thiol–Michael/acrylate hybrid, epoxy/acrylate curable resins, thiol–acrylate/thiol–acetoacetate thermosets, and thiol–ene/epoxy-based polymers [12-14].

UV light sources suffer the drawbacks of being toxic, causing damage to human cells and tissues, besides its limited penetration depth in most materials. For examples, the light penetration of a polystyrene latex ranges from 600 μm at UV light at 400 nm up to 5 cm at near-IR light at 800 nm, and therefore photopolymerization may be applied from thin film coatings to thick samples [14]. Organic dyes used as visible light photosensitizers of polymerization have been extensively studied [15,16], in which high extinction coefficients and their long-living excited states, enabling the photosensitizers to react efficiently with various additives in the photocurable resins. For cost effectiness with long-living excited states, the pioneering works using copper complex in photopolymerization have been developed in 2014 by the group of Lalevée et al. [17,18]. More recently, copper complexes have been used as a new polymerization approach enabling the formation of acetylacetonate radicals by redox reaction with a phosphine and to initiate the free radical polymerization (FRP) of acrylates or the free radical promoted cationic polymerization (CP) of epoxides [19-21].

The efficiency of copper complex (G1) based photoinitiating systems (G1/iodonium salt (Iod)/*N*-vinylcarbazole (NVK) was investigated by Mokbel et al [19] for free radical polymerization (FRP) of acrylates and the free radical promoted cationic polymerization (CP) of epoxides using light source (LEDs at 375, 395, 405 nm, halogen lamp). The roles of G1 concentrations, coating thickness (25μm and 1.4mm), water content, stability of the formulation and hydrolytic stability of the coatings are investigated. The G1/Iod/NVK system was also compared to reference systems based on BAPO (*bis*(2,4,6-trimethylbenzoyl)-phenylphosphineoxide-Irgacure 819), 2-isopropylthioxanthone or anthracene.

This article will present, for the first time, the kinetics and the general conversion features of the 3-initiator, [A], [B] and [N], system based on proposed mechanism of Mokbel et al [19] for both FRP and CP. The roles of co-initiator [B] and [N] including their dual functions of regeneration of initiator [A] and generation of radicals for improved conversion. The key factors influencing the conversion rates and efficacy will be explored by analytic formulas derived from a kinetic model for a 3-initiator and 2-monomer system. Finally, the measured data of Mokbel et al [19] will be quantitatively analyzed by our formulas, rather than their qualitative disccusions.

2. Methods and Modeling Systems

2.1. Photochemical Kinetics

As shown by Figure 1, a 3-initiator system (A/B/N) defined by the ground state of initiator-A, which is excited to its first-excited state PI*, and a triplet excited state T having a quantum yield (q). The triplet state T interacts with initiator [B] to produce an oxodized-A (or [C]) and radical R, which interacts with co-initiator (or additive) N to produce radical S', which couples with [C] to prodcue another radical S and lead to the regeneration of [A]. Monomer M' and M coupled with radicals S' and S for FRP and CP conversion, respetively.

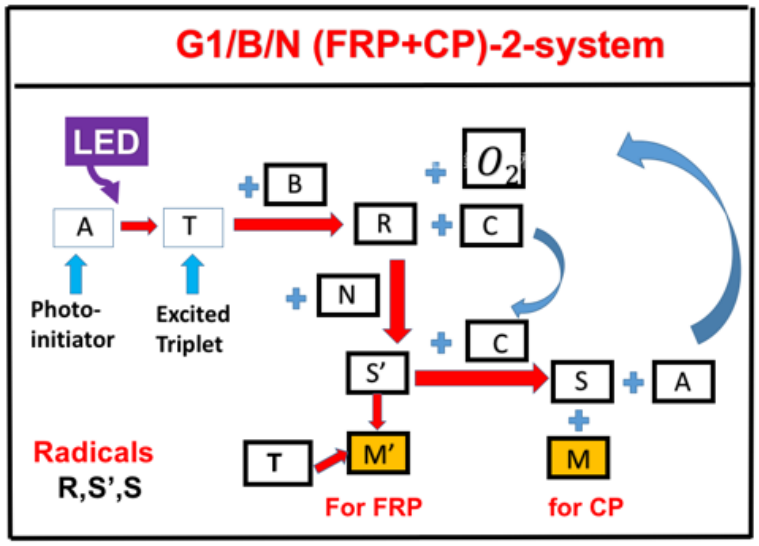

Figure 1. The schematics of a 3-initiator system, (A/B/N), where A is the ground state of initiator-A, having an excited triplet state T, which interacts with co-initiator [B] to produce radical R and oxodized-A (or [C]); R interacts with co-initiator (or additive) N to produce radical S', which couples with [C] to prodcue another radical S and lead to the regeneration of [A]. Monomer M' and M coupled with radicals S' and S for FRP and CP conversion, respectively.

A specific measured system of related to Figure 1 was reported by Mokbel et al [19], in which their Scheme 3 proposed the photoredox catalytic cycle for a 3-component (co-initiator) system of G1/Iod/NVK, where G1 is copper complex in combination with iodonium salt (Iod), (oxidizing agent) generates the radical species through an electron transfer reaction. A propagation system containing the *N*-vinylcarbazole (NVK) additive leads to simultaneous regeneration of G1 and the formation of highly reactive cations (Ph- NVK+), which can very efficiently initiate the CP conversion.

The kinetic equations for our previous systems [22-24] are revised for the 3-initiator (A/B/N) and 2-monomer system (M'M), as follows.

$$\frac{\partial[A]}{\partial t} = -bI[A] + (k_5 + k_1[A])T + k_4[C]S' \quad (1)$$

$$\frac{\partial[B]}{\partial t} = -k_2T[B] \quad (2)$$

$$\frac{\partial[C]}{\partial t} = (k_3T - k_4S')[C] \quad (3)$$

$$\frac{\partial T}{\partial t} = bI[A] - (k_5 + k_1[A] + k_1[B] + k_7M')T \quad (4)$$

$$\frac{\partial R}{\partial t} = k_2[B]\,T - k''R[O_2] - k_6RN \quad (5)$$

$$\frac{\partial N}{\partial t} = -k_6RN \quad (6)$$

$$\frac{\partial S\prime}{\partial t} = k_6RN - (k_4[C] + K'M')S' \quad (7)$$

$$\frac{\partial S}{\partial t} = k_4[C]S' - KSM \quad (8)$$

In Eq. (1) k_4[C]S' is the regeneration (REG) term of of the initiator, [A]. b=83.6$a'wq$, where w is the light wavelength (in cm) and q is the triplet state T quantum yield; a' is the mole absorption coefficient, in (1/mM/%) and I (z, t) is the light intensity, in mW/cm^2. All the rate constants are defined

previously [22] and they are related by the coupling terms. For examples, k_j (with j=1,2,3) are for the couplings of T and [A], [B], and [C], respectively; k_4 and k_6 are for the couplings of S' and [C], and R and M, respectively. The comversion due to coupling of T, and radicals R and S' with monomer M' (for FRP), and S with M (for CP) are given by tye rate constants of k_7, k_6, K' and K' respectively. We have also include the oxygen inhibition effect [23] (for system in air) given by the k"R[O_2} in Eq. (5). For system with laminate or when R is insensitive to oxygen (or k" is very small), oxygen inhibition is redcued and conversion is improved [23]. In above kinetics, we assume the bimolecular termination can be ignired that is no R and R, S'and S , or S and S couplings.

The monomer conversions for FRP and CP are given by [22]

$$\frac{dM'}{dt} = -(k_7T + k_6R + K'S')M' \quad (9)$$

$$\frac{dM}{dt} = -KSM \quad (10)$$

Above equations indicate that conversions for FRP and CP are given by the interaction of (T,R,S') and M', and S and M, respectively. We note that the co-initiator, [B] (or Iod) has dual function of enhancing FRP (via R and S') and CP (via S).

We note that Eq. (1) to (10) are constructed for the specific system of Mokbel et al [xx], using short hand notations: A=Cu(I); T=Cu*(I), B=Iod; N=NVK, C= Cu(II), R= Ar*, S'= Ar-NVK*, S= Ar-NVK$^{(+)}$, in system having two monomers M'=TAMPTA (for FRP conversion) and M=epoxy (for CP conversion), where Iod is iodonium salt , NKV is N-vinylcarbazole, and TAMPA is Trimethylol-propane triacrylate. They also compare the conversion of initiator A=cooper and A= bis(2,4,6-trimethylbenzoyl)-phenylphosphineoxide (BAPO).

For comprehensive modeling we will use the so-called quasi-steady state assumption [15,18]. The life time of the singlet and triplet states of photosensitizer, the triplet state (T), and the radicals (R, S' and S), since they either decay or react with cellular matrix immediately after they are created. Thus, one may set dT/dt=dR/dt=dS'/dt = dS/dt= 0, which give the quasi-steady-state solutions: T=bIg[A], R= k_2bIgg'[A][B], S'= (k_6bIg[A][B] - k"g'[B][O_2])/[(k_4 C+K'M'); S= k_4[C]S'/(KM); and g=1/(k_5+ k_1[A]+k_2[B]+k_7M'), g'=1/(k"[O_2] +k_6N). The oxygen inhibition effect, included in g' and S', reduces the free radicals, R and S', and hence the conversion of FRP and CP if system is in air.

Under the above quasi-steady-state solutions, we obtain the simplified equations as follows.

$$\frac{\partial[A]}{\partial t} = -bIg[A](k_2[B] + k_7M') + REG \quad (11)$$

$$\frac{\partial[B]}{\partial t} = -k_2bIg[A][B] \quad (12)$$

$$\frac{\partial[C]}{\partial t} = bIg[A]\,(k_3[C] - k_6[B]) \quad (13)$$

$$\frac{\partial N}{\partial t} = -k_6RN \quad (14)$$

where the initiatior-A regeneration term is given by REG=k_4[C]S', in Eq. (11). We note that this REG enhances the conversion of FRP and CP, serving as a catalytic cycle.

The equation for the FRP and CP conversion rate functions are given by

$$\frac{dM'}{dt} = -R'_TM' \quad (15)$$

$$\frac{dM}{dt} = -k_4[C]S' \quad (16)$$

where R_T is the rate fucniton of FRP given by $R'_T=bIg[A](k_7+k_2k_6g'[B])+K'S'$, The conversion efficacy of FRP is defined by $C_V=1- M/M_0 = 1- \exp(-E)$, where the E function is given by the time integral of the rate functions, R_T. However, the conversion efficacy of CP $C'_V=1- M'/M'_0$ is defined the time integral of Eq. (16).

The dynamic light intensity is givenby [22]

$$\frac{\partial I(z,t)}{\partial z} = -A'(z,t)I(z,t) \quad (17)$$

$$A'(z,t) = 2.3[(a'-b')[A] + b'[[A]_0 + q'] \quad (18)$$

where, a' and b' are the molar extinction coefficient (in 1/mM/%) of the initiator and the photolysis product, respectively; q' is the absorption coefficient of the monomer. Most previous modeling assumed a constant [A] in Eq. (18).

3.. Results and discussion

A full numerical simulation is required for the solutions of Eq. (11)-(17), which will be presenetd elasewhere. We will focus on comprehensive analysis for many features and the enhancement effects related to the measured data of Mokbel et al [22], based on the analytic solutions.

3.1 Analytic results

For the case that oxygen effect is ignored, using our previously developed approximated analytic formulas [22] for the light intensity and solving for Eq. (11)-(14), we obtain the expresive forms

$$I(z,t) = I_0\, exp[\,-A'(z,t)z] \quad (19)$$

$$[A](z,t) = [A]_0\ exp[-F'B'(z,t)t] \quad (20)$$

$$[B](z,t) = [B]_0 - E(z,t) \quad (21)$$

$$N(z,t) = [N]_0 - E(z,t) \quad (22)$$

$$E(z,t) = [bI_0[A]_0/(F'B')]\,[1 - exp(-F'B't)] \quad (23)$$

$$A'(z,t) = A'_0 - b'(z)t \quad (24)$$

Where $F'=1-(k_6/k_2)$, $A'_0=2.3(a'[A]_0+q')$, $B'(z)= bI_0\exp(-A''z)$, $b'(z)=2.3(a'-b')bzI_0[A]_0$, with A'' is the averaged absorption given by $A''=1.15(a'+b')[A]_0+2.3q$. We note that the –B't term represents the decrease of A', or increase of light intensity due to the initiator [A] depletion. Eq. (19) is the approximated solution of Eq. (17) with oxygen inhibition term is ignored (or $k''R[O_2]=0$). In deriving Eq (20), we also assue that $k_2[B] << k_5+k_7M'$, such that $g=1/(k_2B)$; $k_6[C] >> k_9M$, and $k_2[B] >> k_7M'$ such that the regeneration term $REG= k_4[C]S'= (k_6/k_2)bI[A]$.

For strong REG (or when k_6 comparable to k_2), [A] is almost a constant, i.e., $[A]=[A]_0$.. In this case, anaytic solution of Eq. (16) and (17) give the conversion of FRP and CP defined by $C'_V=1-M'/M'_0 = 1- \exp(-E)$, $C_V=1-M/M_0$; where the E(t) function are given by the time integral of the rate functions, $R'_T = bI_0[A][(k_7/k_2)/[B]+ 1/N+ K'k_6/(k_2\, k_4[C])\,]$, for FRP which requires numerical integration. However, CP conversion given by the time integral of $R_T=bIg[A][B]=bI[A](1-(k_1/k_2)[A]/[B]$, with the approximated Eq. (20) and (21), can be obtained analytically as follows.

$$C_V = bI_0 exp(-A'_0 z)[A]_0\,(1 - k_1/(k_2[B]_0)\,Q(z,t) \quad (26)$$

$$Q(t) = [1 - exp(-F'B't)]/(F'B') \quad (27)$$

which has a transient state (for small time) given by $C_V=GbtI_0[A]_0$, with $G(z)=(1-k_1/(k_2[B]_0)\exp(-A'_0z)$, and steady-state given by , when $Q(t)=1/(F'B')$, $C_V=GbI_0[A]_0/(F'B')$; with $F'=1-(k_6/k_2)$, $B'(z)= bI_0 \exp(-A''z)$ and $A''=1.15(a'+b')[A]_0+2.3q$.

Dark reaction is defined by the time the light is turned off (at *t=ti*), and the concentration of the initiator [B(t)], or Q(t)-function, remains virtually unchanged in time, i.e., Q(t≥ti) =constant, and the CP conversion for dark polymerization is given by Eq. (26), but with

$$Q(t - ti) = [1 - exp[-F'B'(t - ti)]/(F'B') \quad (28)$$

3.2 General features and new findings

As shown by Eqs. (15) and (16), and the approximated solution of Eq. (19) to (27), the following significant features of the 3-initiator system A/B/N are summarized.

(a) Co-initiator [B] has multiple functions of : (i) regeneration of initiator [A] leading to higher FRP and CP conversion; (ii) generation of radical S' for CP conversion, both are via $k_6bIg[A][B]$. The regeneration term given by $REG= k_4[C]S'= bIg[A][B]$, with a REG factor $F'=1-(k_6/k_2)$ in Eq. (26). For strong regeneration, (or when k_6 comparable to k_2), the reduction factor $F'=1-(k_6/k_2)$ reduces the depletion of initiator [A], and improves the CP conversion, Eq. (26). For the extreme case of F'=0, depeltion of [A] due to light is totally compensated by the REG term, d[A]/dt=0, and $[A]=[A]_0$, shown by Eq. (20).

(b) Co-initiator [N] has functions of : (i) generation of S' for FRP; (ii) generation of cationic radical S for CP conversion; via $k_6R[N]$. We note that [N] always enhances steady-state FRP, via $bI_0[A]_0N_0/(k_5)[k_2[B]_0+(k_7+K'[B]_0/N_0)]$, which has 3 contributions, from $[A]_0[B]_0N_0$ and $(k_7+K'[B]_0)/N_0$; however, steady-state CP conversions is independent to [N], given by Eq. (26).

(c) Dark polymerization is given by Eq. (28), which provides the CP conversion even after the light is turned off. The lack of a termination mechanism for the CP conversion via the cationic intermediates which enables the polymerization to continue in living mode without requiring a constant input of light for propagation, thus offers an extended dark-cure reactions. Such kinetic behavior contrasts with that of the radical-mediated pathway of FRP, where radical and monomer reactions are almost immediately interrupted due to the effective exhaustion of the reactive radical intermediates. This dark polymerization also exists in thiol–Michael additions [13], but not in thiol–ene additions [14].

(d) The oxygen inhibition effect ($k''[O_2]$), included in $S'=(k_6bIg[A][B] - k''[O_2])/[(k_4[C]+K'M')$, which reduces the free radicals S', and thus the FRP conversion is lower in air comparing to in laminate [24].

(e) For thick polymers, the light intensity and the initiators concentrations are decreasing function of the depth (z), as shown by $G(z)=(1-k_1/(k_2[B]_0)\exp(-A'_0z)$. However, light intensity is an increasing function of time (t) due to the depletion of [A], unless for the extreme case that F'=0 (a total compensation). Detailed temporal and spatial profile of conversion function require extensive numerical simulation which was published elsewhere [22,26].

3.3. Synergic effects

As reported by van der Laan et al. [7], the effectiveness of a photoinhibitor in a two-color system is strongly monomer-dependent, which also requires: (i) a high conversion of blue-photoinitiation in the absence of the UV-active inhibitor; (ii) a strong chain termination with significant reduction of blue and UV conversion

in the presence of UV-active inhibitor and (iii) short induction time or rapid elimination of the inhibitor species in the dark (or absence of UV-light). Conversion efficiency may be also improved by reduction of the oxygen inhibition effect [9,10,25]. Synergic effects have been reported using co-initiator and/or additives [26-30], and 2- and 3-wavelength systems [31-33]. The present article present the kinetics analysis of the co-initiator enhanced (catalyzed) conversion in FRP and CP which was reported by Mokbel et al [19], Garra et al [20] and Noribnet et al [21] in the 3-compnent G1/Iod/NVK system.

3.4 Analysis of measured results

Besides the general features described in section 3.2, our analytical formulas may be also used to analyze the measured results of Mokbel et al [19] as follows.

(a) Fig. 2 and Fig. 5 of Mokbel et al [19] for CP profiles of various epoxy functions, showning that G1/Iod/NVK has the faster raising rate and higher steady-state value than that of BAPO/Iod/NVK having a lower light absortion. This feature may be quantitatively and precisely anaylyzed by our Eq. (26), in which the conversion and rate fucntion is proportional to the factor $bI_0[A]_0\,[1-k_1/(k2[B]_0)]$, which is an increasing function of the light absoprtion coefficient and the co-initiator concentrations $[A]_0$ and $[B]_0$; where $b=83.6a'wq$, where a' is the molar extinction coefficient, w is the UV light wavelength and q is the triplet state quantum yield.

(b) Fig. 3 of *Mokbel* et al [19] showed that higher dark polymerization in G1/Iod/NVK than BAPO/Iod/NVK. This feature may be easily seen by our Eq. (26) and (28), which are increasing function of the the molar extinction coefficien. The dark polymerization exists in the free radical promoted CP and in Thiol–Michael addition polymerization [13], but does not exist in one-initiator FRP systems.

(c) Fig. 4 and Fig. 7 of Mokbel et al [19] showed the effects of G1 concentration and sample thickness (24 μm and 1.4 mm). In the case of thick samples (1.4mm) (Figure 4B), the CP conversion in G1/Iod/NVK system increases when decreasing the photoinitiator concentration, in contract to that of thin sample that higher concentration has higher conversion. These features may be analyzed by our thick polymer formula: $I(z)= I_0 \exp(-A''z)$, with $A''=1.15(a'+b')[A]_0$, which shows that increasing the concentration, $[A]_0$, (or larger A") for thick sample (with z=1.4 mm), the penetration of the light decreases, as shown by Eq. (19) and (26). For very thin sample (with z=25 μm), A"z=0, and $I(z)= I_0$, independent to $[A]_0$. Therefore, there is an optimal initiator concentration in thick samples. We have previously [22] demonstrated mathematically the optimal $[A]_0$ value given by dG/dz=0, with $G=[A]_0 \exp(-bzI_0[A]_0)$, to obtain the optimal concentration $[A]^*=1/(bz\,I_0)$ which is inverse proportional the product of light intnesity(I_0), absorption coefficient (b) and the sample thickness (z). In contrast, for very thin sample, the conversion is always higher for higher $[A]_0$ and/or $[B]_0$ and there is no optiomal values.

(d) Fig. 12 and 14 of Mokbel et al [19] showed the oxygen inhibition effects (OIE) for system in air and in lamine. They showed that the FRP conversion of TMPTA was higher in laminate than in air. In contrast, the CP conversion of epoxy function was lower in laminate than in air. It may be because the FRP of TMPTA was faster than the CP, and most of the free radicals were consumed

to initiate FRP. We also note that the radical for CP is much less sensitive to OIE than that of FRP. The participation of different thermal effects between thin and thick samples can also participate to some extend to explain the difference of behavior between CP and FRP. Mathematically, this features are shown by our formula for FRP free radical given by $S'=(k_6bIg[A][B] - k''[O_2])$, *in which* $k''[O_2]=0$, in laminate. Our formulas also predicts that thick sample has less O_2 supply (inside the sample), such that OIE is smaller than that of thin sample. However, the FRP "volume" conversion of thick sample is still lower than thin sample due to the stronger light absorption loss in thick sample (the Beer-Lamert law), as shown by Fig. 14 (A) and (B) of Mokbel et al [19].

(e) Fig. 14 of Mokbel et al [19] also showed that the addition of the Boltorn H2004 resin in the UviCure S105/TMPTA blend 15 improves the final epoxy functio. They explained as the decrease of cross-link density leading to a higher mobility of the reactive species. Lin at al [24] has developed a modeling for the role of oxygen inhibition and viscosity, in which lower viscosity (or higher mobility) leads to higher conversions. As also proposed by Wu et al [35], the rate parameters is a decreasing function of the efficacy.

4. Conclusion

This article presents, for the first time, the kinetics and the general conversion features of a 3-initiator ([A], [B] and [N]) system, based on proposed mechanism of Mokbel et al [19], for both free radical polymerization (FRP) of acrylates and the free radical promoted cationic polymerization (CP) of epoxides. Higher conversion of FRP and CP can be achieved by co-initiators [B] and [N], via the dual function of (i) regeneration of photoinitiator [A], and (ii) generation of extra radicals S' and S. The FRP and CP conversion is proportional to, respectively, the nonlinear and linear power of bIg[A][B]. Because of oxygen inhibition effects (OIE), system in air has lower conversion than in lamine. For thick samples, there is an optimal initiator concentration for [A] which is inverse proportional (bzI_0), or the product of light intnesity(I_0), absorption coefficient (b) and the sample thickness (z). In contrast, for very thin sample, the conversion is always higher for higher concentration $[A]_0$ and/or $[B]_0$ and there is no optiomal values. The feature of dark polymerization, given by Eq. (28), in CP conversion enables the polymerization to continue in living mode without requiring a constant input of light for propagation, in contrasts with that of the radical-mediated pathway in most conventional FRP. The measured results of Mokbel et al [22] are well analyzed and matching the predicted features of our modeling.

Funding: The Agence Nationale de la Recherche (ANR agency) is acknowledged for its financial support through the NoPerox grant.

Acknowledgments: JTL thanks the internal grant of New Vision Inc. and DCC thanks the financial support from 359 China Medical University with the grant number CMU109-S-39.

Conflicts of Interest: Jui-Teng Lin is the CEO of New Vision Inc.

References

1. Fouassier, J. P. & Lalevée, J. Photoinitiators for Polymer Synthesis-Scope, Reactivity and Efficiency. Wiley-VCH Verlag GmbH & Co. KGaA: Weinheim, Germany, 2012.

2. Yagci, Y., Jockusch, S. & Turro, N.J. Photoinitiated polymerization: Advances, challenges and opportunities. *Macromolecules* **43**, 6245–6260 (2010).
3. Ligon, S.C.; Liska, R.; Stampfl, J.; Gurr, M.; Mulhaupt, R. Polymers for 3D printing and customized additive manufacturing. *Chem. Rev.* **2017**, *117*, 10212−10290.
4. Shusteff, M.; Browar, A.E.M.; Kelly, B.E.; Henriksson, J.; Weisgraber, T.H.; Panas, R.M.; Fang, N.X.; Spadaccini, C.M. One-step Volumetric Additive Manufacturing of Complex Polymer Structures. *Sci. Adv.* **2017**, *3*, 7.
5. Kelly, B.E.; Bhattacharya, I.; Heidari, H.; Shusteff, M.; Spadaccini, C.M.; Taylor, H.K. Volumetric Additive Manufacturing via Tomographic Reconstruction. *Science* **2019**, *363*, 1075−1079.
6. de Beer, M.P.; van der Laan, H.L.; Cole, M.A.; Whelan, R.J.; Burns, M.A.; Scott, T.F. Rapid, Continuous Additive Manufacturing by Volumetric Polymerization Inhibition Patterning. *Sci. Adv.* **2019**, *5*, 8.
7. van der Laan, H.L.; Burns, M.A.; Scott, T.F. Volumetric Photopolymerization Confinement through Dual-Wavelength Photoinitiation and Photoinhibition. *ACS Macro Lett.* **2019**, *8*, 899–904.
8. Childress, K.K., Kim, K., Glugla, D.J., Musgrave, C.B., Bowman, C.N. & Stansbury, J.W. Independent control of singlet oxygen and radical generation via irradiation of a two-color photosensitive molecule. Macromolecules **52**(13):4968–4978 (2019).
9. Scott, T.F.; Kowalski, B.A.; Sullivan, A.C.; Bowman, C.N.; McLeod, R.R. Two-Color Single-Photon Photoinitiation and Photoinhibition for Subdiffraction Photolithography. *Science* **2009**, *324*, 913–917.
10. Kirschner, J.; Paillard, J.; Bouzrati-Zerell, M.; et al. Aryliodonium ylides as novel and efficient additives for radical chemistry: example in camphorquinone (CQ)/Amine based photoinitiating systems. *Molecules* **24**(16), 2913 (2019); doi:10.3390/molecules24162913.
11. Bonardi AH,; Dumur F,; Grant TM,; et al. High performance near-Infrared (NIR) photoinitiating systems operating under low light intensity and in the presence of oxygen. Macromolecules, 2018, 51, 1314-1324.
12. Claudino,M.; Zhang,X.; Alim,M.D.;Podgórski,M.;Bowman, C. N. Mechanistic Kinetic Modeling of Thiol-Michael Addition Photopolymerizations via Photocaged “superbase” Generators: An Analytical Approach. Macromolecules 2016, 49 (21), 8061−8074.
13. Huang, S.; Sinha, J.; Podgorski, M.; Zhang, X.; Claudino M. Bowman, C.N. Mechanistic modeling of the Thiol−Michael addition polymerization kinetics: Structural effects of the Thiol and Vinyl monomers. *Macromolecules* **2018**, *51*, 5979–5988.
14. Chen, K.T.; Cheng, D.C.; Lin, J.T.; Liu, H.W. Thiol-Ene photopolymerization in thick polymers: kinetics and analytic formulas for the efficacy and crosslink depth. *Polymesr. 2019,* **11**, 1640 . doi:10.3390/polym11101640.
15. Noirbent, G.; Dumur, F. Recent advances on naphthalic anhydrides and 1,8-naphthalimide-based photoinitiators of polymerization. *Eur. Polym. J.* **2020**, *132*, 109702.
16. Pigot, C.; Noirbent, G.; Brunel, D.; Dumur, F. Recent advances on push-pull organic dyes as visible light photoinitiators of polymerization. *Eur. Polym. J.* **2020**, *133*, 109797.

17. Alzahrani, A.A.; Erbse, A.H.; Bowman, C.N. Evaluation and development of novel photoinitiator complexes for photoinitiating the copper-catalyzed azide-alkyne cycloaddition reaction. *Polym. Chem*. **2014**, *5*, 1874–1882.
18. Xiao, P.; Dumur, F.; Zhang, J.; Fouassier, J.-P.; Gigmes, D.; Lalevée, J. Copper complexes in radical photoinitiating systems: Applications to free radical and cationic polymerization under visible lights. *Macromolecules* **2014**, *47*, 3837–3844.
19. Mokbel, H.; Anderson, D.; Plenderleith, R.; Dietlin, C.; et al. Copper photoredox catalyst "G1": A new high performance photoinitiator for near-UV and visible LEDs. *J. Polym. Chem*. **2017**, *8*, 5580–5592.
20. Garra, P.; Dietlin, C.; Morlet-Savary, F.; Dumur, F.; et al Redox two-component initiated free radical and cationic polymerizations: Concepts, reactions and applications. Progress in Polymer Science, 2019, 94, pp.33–56. 10.1016/j.progpolymsci.2019.04.003
21. Noirbent, G.; Dumur, F. Recent Advances on Copper Complexes as Visible Light Photoinitiators and (Photo) Redox Initiators of Polymerization. Catalysts, MDPI, 2020, 10, 10.3390/catal10090953 .
22. Lin, J.T,; Cheng, D.C. Modeling the efficacy profiles of UV-light activated corneal collagen crosslinking. PloS One. 2017;12:e0175002.
23. Lin, J.T. Kinetics of Enhancement for Corneal Cross-linking: Proposed Model for a Two-initiator System. Ophthalmology Research, 2019, 10(3): 1-6; Article no.OR.49970 DOI: 10.9734/OR/2019/v10i330109.
24. Lin, J.T,; Chen. K.T,; Cheng. D,C,; Liu. H,W. Modeling the efficacy of radical-mediated photopolymerization: the role of oxygen inhibition, viscosity and induction time. *Front. Chem. 2019, 7:760. doi: 10.3389/fchem.2019.00760.*
25. *Lin, .JT.; Liu, H.W.; Chen, K.T.; Cheng, D.C.* Modeling the optimal conditions for improved efficacy and crosslink depth of photo-initiated polymerization. Polymers. 2019, 11, 217; doi:10.3390/polym11020217.
26. Lin J.T.; Liu HW,; Chen KT,; Chiu YC, ; Cheng DC. Enhancing UV photopolymerization by a red-light pre-irradiation: kinetics and modeling strategies for reduced oxygen-inhibition. J Polymer Science, 2020，58， 683-691，DOI:10.1002/pol.20190201.
27. Mira, A.; Hijazi,A.; Lin, J.T.; Graff, B.; Dumur, F.; Lalevee, J. Coumarin Derivatives as Photoinitiators in Photo-Oxidation and Photo-Reduction Processes and a Kinetic Model for Simulations of the Associated Polymerization Profiles. App Polymer Material. 2020, 2,2769-2780.
28. Lin, J.T,; Lalevee, L.; Cheng. D,C. Synergetic kinetics of free radical and cationic photopolymerization in three co-initiators and two-monomers system. Polymers (2021, in press).
29. Chen, KT, Cheng, DC Lin, JT, Liu, HW. Thiol-Ene photopolymerization: Scaling Law and Analytic Formulas for Conversion based on Kinetic-rate and Thiol-ene Molar-ratio. Polymers 2019, 11, 1640; doi:10.3390/polym11101640.

30. Chiu, Y.C.; Cheng, D.C.; Lin, J.T.; Chen, K.T.; Liu, H.W. Dual-function enhancer for near-infrared photopolymerization: kinetic modeling for improved efficacy by suppressed oxygen inhibition. IEEE Access, 2020, 8, 83465-83471.
31. Lin J.T.; Chen K.T.; Cheng D.C.; Liu, H,W. Dual-wavelength (UV and Blue) controlled photopolymerization confinement for 3D-printing: modeling and analysis of measurements. Polymers, 2019, 11, 1819.
32. Lin, J.T.; Liu, H.W.; Chen, K.T.; Cheng, D..C. 3-wavelength (UV, blue, red) controlled photopolymerization: improved conversion and confinement in 3D-printing. IEEE Access, 2020, 8, 49353-49362.
33. Lin, J.T.; Chen, K.T.; Cheng D.C.; Liu, H,W. Enhancing blue-light-initiated photopolymerization in a three-component system: kinetic and modeling of conversion strategies. J Polymer Research, 2021, 28:2.
34. Wu, J.; Zhao, Z.; Hamel, C.M. et al. Evolution of material properties during free radical photopolymerization. J Mechan Phys Solid. 2018, 112, 25-49.